Time resolved scanning Kerr microscopy of hard disk writer structures with a multilayered yoke

W. Yu, P. Gangmei, P. S. Keatley, R. J. Hicken, M. A. Gubbins, P. J. Czoschke, and R. Lopusnik

Citation: Applied Physics Letters **102**, 162407 (2013); doi: 10.1063/1.4802977
View online: http://dx.doi.org/10.1063/1.4802977
View Table of Contents: http://scitation.aip.org/content/aip/journal/apl/102/16?ver=pdfcov
Published by the AIP Publishing

Time resolved scanning Kerr microscopy of hard disk writer structures with a multilayered yoke

W. Yu,[1] P. Gangmei,[1] P. S. Keatley,[1] R. J. Hicken,[1] M. A. Gubbins,[2] P. J. Czoschke,[3] and R. Lopusnik[3]
[1]*School of Physics, University of Exeter, Stocker Road, Exeter EX4 4QL, United Kingdom*
[2]*Research & Development, Seagate Technology, 1 Disc Drive, Springtown Industrial Estate, Derry BT48 0BF, Northern Ireland*
[3]*Recording Heads Operation, Seagate Technology, 7801 Computer Avenue South, Bloomington, Minnesota 55435, USA*

(Received 18 December 2012; accepted 11 April 2013; published online 24 April 2013)

Partially built hard disk writer structures with a multilayered yoke formed from 4 repeats of a NiFe(∼1 nm)/CoFe(50 nm) bilayer were studied by time and vector resolved scanning Kerr microscopy. Dynamic images of the in-plane magnetization suggest an underlying closure domain equilibrium state. This state is found to be modified by application of a bias magnetic field and also during pulse cycling, leading to different magnetization rotation and relaxation behavior within the tip region. © *2013 AIP Publishing LLC* [http://dx.doi.org/10.1063/1.4802977]

Increased write head fields with repeatable picosecond rise and fall times are required to increase storage densities and bit rates within perpendicular magnetic recording (PMR) technology, while avoiding erase after write[1] (EAW) phenomena and popcorn noise.[2] The pole tip, yoke, and confluence region together constitute a complex 3 dimensional object, and advanced measurement techniques have been developed to characterize its non-uniform magnetic state.[3] Previous experimental studies[4–9] of the rise time and remanent value of the write field have concentrated on the pole tip region. However, the magnetization dynamics within the yoke have a significant impact upon the amplitude and temporal form of the write field generated by the pole tip. Current understanding of yoke dynamics is derived mainly from simulations.[10] In a recent study,[11] time resolved scanning Kerr microscopy (TRSKM) was used to simultaneously detect all three spatial components of the magnetization within a writer structure with a single layer yoke subject to a bias field. Time resolved images confirmed the occurrence of flux beaming,[12] where magnetic flux is concentrated along the symmetry axis of the yoke during dynamic operation of the writer, demonstrating that TRSKM can directly image the dynamic response of the writer.

In this study, writer structures with a multilayered yoke were excited with high-frequency current waveforms of different polarities, and with different bias magnetic fields to empirically determine and understand the static and dynamic states of the writer magnetization under conditions similar to those experienced in a hard disk drive. In contrast to Ref. 12, the upper layer of the yoke exhibits a clear flux closure state, and a richer variety of dynamic behavior is observed. The equilibrium state magnetization within the tip region of the writer is found to be complicated, being influenced by the bias field and the polarity of the driving current, in some cases with indications that EAW may be significant.

The sample consisted of a partially built writer structure with yoke and pole tip formed from 4 repeats of a NiFe(∼1 nm)/CoFe(50 nm) bilayer designed to possess a high moment and low coercive field. The geometry of the yoke, pole tip, and coil windings shown in Figure 1(a) is identical to that in Ref. 10. The three coil turns, labeled C1, C2, and C3, lie between the top and bottom layers of the yoke and generate an in-plane driving field when current is applied.

The schematic layout of the TRSKM is shown in Figure 1(b) and has been described in detail previously.[10] The pulse used to excite the writer had 1.6 ns duration and 11.2 V amplitude since larger values led to signals that had noticeable stochastic character.[11,13] The response of the yoke was probed by a laser pulse of 100 fs duration focused onto its surface by a × 60 microscope objective lens. A bias magnetic

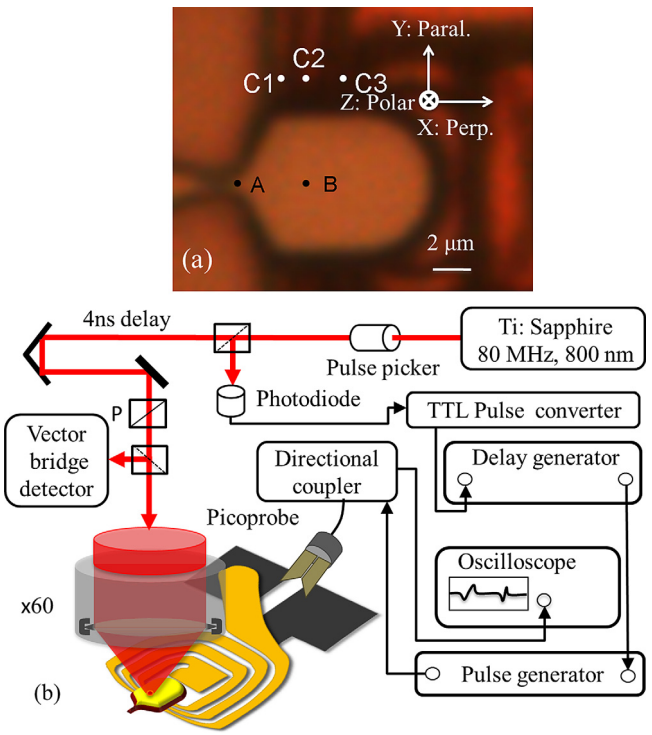

FIG. 1. (a) Wide field optical microscope image of the sample. C1, C2, and C3 are the coil turns. A and B are positions where time resolved signals were recorded. (b) The experimental set-up.

field was applied in the plane of the yoke and perpendicular to its axis of symmetry. The back-reflected optical pulse was directed into a quadrant photodiode polarization (vector) bridge.[14] The vector bridge was used to simultaneously detect the total reflected optical intensity (refl.), the in-plane magnetization components parallel (paral.) and perpendicular (perp.) to the bias field, and the out of plane magnetization component (polar). Due to the optical skin depth effect, only the upper surface region of the upper layer of the yoke was probed by the TRSKM.

Measurements were first performed without a static bias magnetic field. Figure 2(a) shows time resolved signals acquired from position B in Figure 1(a), while Figures 2(b) and 2(c) show dynamic images taken at the time delays indicated in Figure 2(a). While the magnetic images appear less sharp than the reflectivity image, they were acquired simultaneously, suggesting that the dynamic magnetization indeed varies gradually with position. The direction of the pulsed current I_p is shown in each panel. The polarity of the time resolved signals, and the contrast within the perpendicular and polar channels of the dynamic images, is seen to reverse with the polarity of the pulsed current as expected. However, in Figure 2(a), the parallel channel in the upper panel shows a constant value during the whole 4 ns scan, while a clear time dependent response to the pulsed current is seen in the parallel channel in the lower panel. The shapes of the signals observed in the perpendicular and polar channels also show definite but less dramatic differences between the upper and lower panels, for opposite current polarity. Surprisingly, the contrast in the polar channel, within Figures 2(b) and 2(c), shows the same polarity to the left and right of the coil windings even though the driving field is out of plane with opposite polarity. The polar contrast above the coil windings is somewhat weaker since the driving field lies in the plane. Comparison of Figures 2(b) and 2(c) reveals an almost identical distribution of contrast within the parallel channel as the current polarity is reversed. This can be understood if the static magnetization forms stripe domains with magnetization alternating between the up and down directions in adjacent domains. The magnetic field generated above the coil windings lies parallel to the symmetry axis of the yoke and points to the left or right depending upon the polarity of the current. In either case, the magnetization attempts to rotate parallel to the horizontal field, leading to a similar change in the vertical magnetization component regardless of the current polarity. Since the parallel channel images show the change in the vertical magnetization component, light and dark stripes correspond to the magnetization rotating from +/−Y directions. The parallel channel images at negative time delay, 0.3 ns in Figure 2(b) and 0.34 ns in Figure 2(c), show weaker contrast at the right compared to the center of the yoke, suggesting a significantly different relaxation behavior at different positions within the yoke. Strong contrast is also observed in the parallel channel within the tip region at negative delay in Figure 2(b), but not in Figure 2(c), indicating a different equilibrium state and different relaxation behavior within the tip region for different current polarities.

The perpendicular channel in Figure 2(b) shows no contrast within the tip region throughout the 4 ns time scan. However, strong contrast appears within the tip region in the perpendicular channel in Figure 2(c) from 1.04 ns onwards and is still present at 3.46 ns after the driving current has been switched off, suggesting a potential EAW problem. Taken together with the contrast observed in the parallel channel in Figures 2(b) and 2(c), this indicates a complex equilibrium state magnetization distribution and tip response for different current polarities. The perpendicular channel images at 1.9 and 2.6 ns in Figure 2(b) and 1.04, 1.66, 2.28, and 2.7 ns in Figure 2(c) show that the maximum contrast appears within the upper and lower parts of the yoke, respectively. This indicates that the equilibrium state magnetization is not exactly vertical but is canted so as to lie parallel to the edge of the yoke within the confluence region. In Figure 2(b), where the current flows along −Y, the maximum contrast appears in the upper part of the yoke because the static magnetization is canted towards the right and so must rotate further to align with the driving field that points to the left. By similar reasoning, in Figure 2(c), where the driving current instead flows along +Y, the driving field points to the right, and the magnetization must rotate through a larger angle in the lower part of the yoke, leading to stronger contrast in the perpendicular channel. The perpendicular channel in Figure 2(b) at 3 and

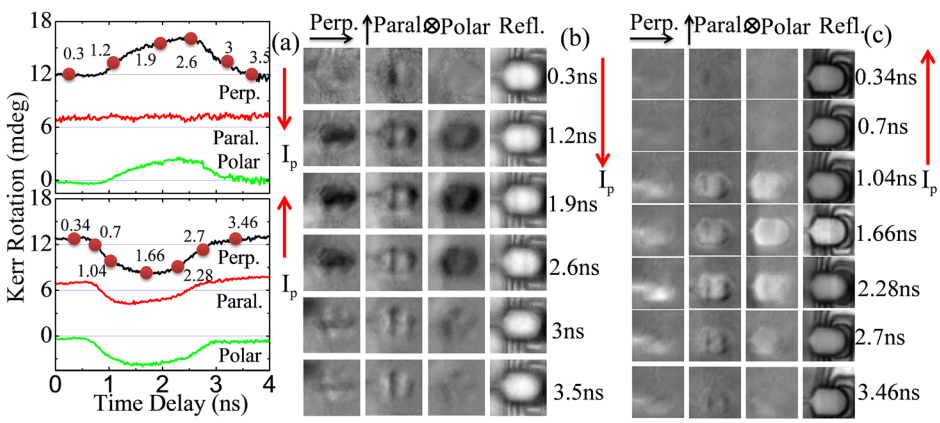

FIG. 2. (a) Time resolved signals acquired from position B in Figure 1(a). The direction of the pulsed current within the current windings I_p for the upper and lower panel is shown. (b) and (c) Dynamic images obtained from the 4 detector channels defined in the main text with I_p flowing downwards and upwards, respectively. For a particular channel, the contrast is normalized to the maximum Kerr amplitude observed within that time series. Black/white corresponds to the dynamic magnetization lying in the −/+ *z*-direction, −/+ *x*-direction, and +/− *y*-direction for the polar, perpendicular, and parallel channels, respectively. The Cartesian axes are defined within Figure 1(a) and shown above the columns in panels (b) and (c).

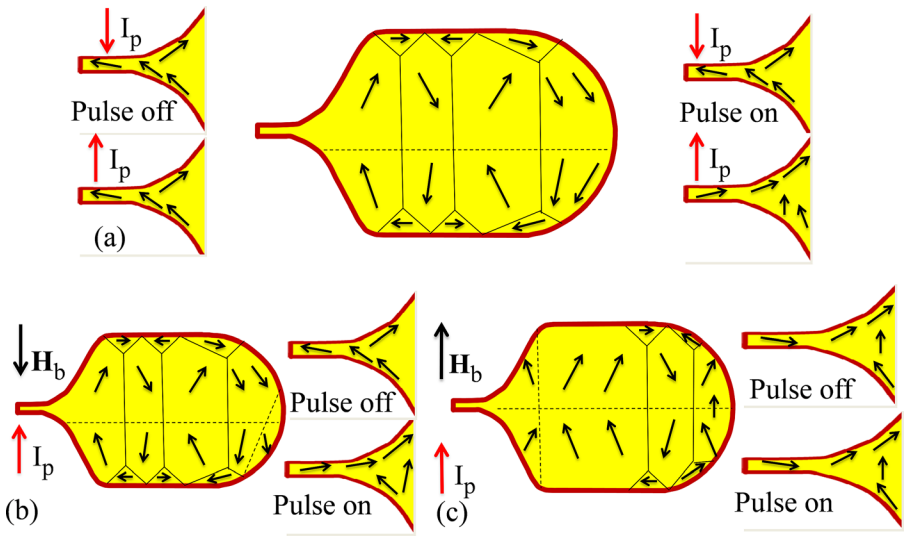

FIG. 3. Sketches of proposed equilibrium states. The dashed lines delineate regions with different canting directions. There is no bias field $\mathbf{H}_b$ applied in (a), while $\mathbf{H}_b$ is applied in the −Y and +Y directions in (b) and (c), respectively. Metastable states of the tip during pulse cycling are inset with the polarity of the pulsed current I_p shown.

3.5 ns shows a dark horizontal band reminiscent of "flux beaming" superimposed on a "chequer board" type background. This occurs after the driving field has begun to fall, suggesting a different rate of relaxation across the area of the yoke. A completely different relaxation behavior is observed in Figure 2(c). The central horizontal band and chequer board background are not observed, and strong contrast is instead observed in the lower part of the yoke.

Based on the dynamic images from the perpendicular and parallel channels, a putative equilibrium state that occurs during the pulse cycling has been sketched in Figure 3(a). The yoke contains two closure domain structures. The magnetization within the large stripe domains lies principally in the vertical direction as a result of induced anisotropy from wafer-level processing. The magnetization within each domain is canted differently within the upper and the lower parts of the yoke so as to be parallel to the edges at the right and left hand ends of the paddle. Proposed metastable equilibrium states within the tip region during repeated pulsing are inset in Figure 3(a) and are seen to depend upon the current polarity.

To obtain a better understanding of the equilibrium state and relaxation behavior, a bias field of 200 Oe was applied orthogonal to the symmetry axis of the yoke. Figure 4(a) shows the time resolved signals obtained from position B for both of the field polarities. The direction of the current was along +Y axis in all cases. Surprisingly, the strongest contrast is observed within the lower part of the yoke in the perpendicular channel in both cases, and a stripe domain structure continues to be observed within the parallel channel. This indicates that the 200 Oe bias field is insufficient to make the equilibrium state uniform.

The perpendicular channel in Figure 4(b) shows clear contrast within the tip region at 1.7, 2.44, 3.02, and 3.86 ns, but the contrast within the same region is very weak for the perpendicular channel in Figure 4(c).

The parallel channel signals in Figure 4(a) show a significant offset which appears as a dark background in the parallel channel images of Figures 4(b) and 4(c). This is most likely the result of mechanical vibration since the bias field exerts a force upon the coil windings when current is supplied. Figure 4(c) shows a black stripe parallel to the bias field at the right end of the yoke for the full range of delay and a weaker dark region close to the tip. Within Figure 4(b), the distribution of contrast is more similar to that in Figures 2(b) and 2(c) with 2 stripes along Y axis appearing at the center and right hand end of the yoke. The polar channel images within Figures 4(b) and 4(c) are almost identical,

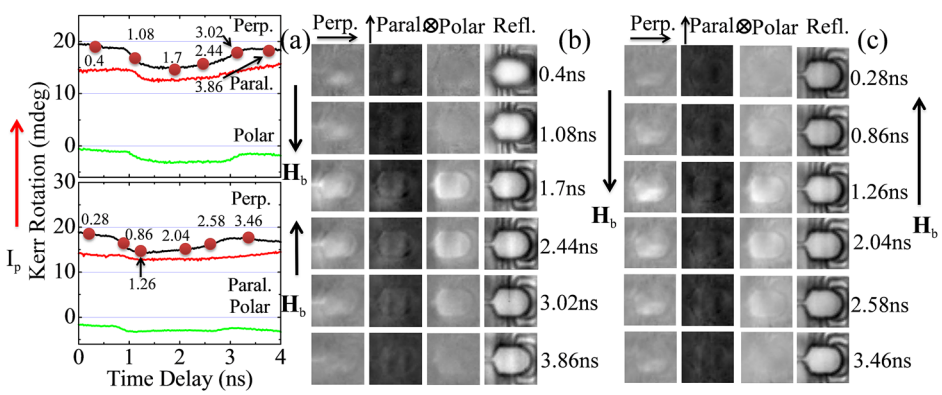

FIG. 4. (a) Time resolved signals acquired from position B in Figure 1(a). The direction of the bias field $\mathbf{H}_b$ for the upper and lower panel is shown. (b) and (c) Dynamic images obtained from the 4 detector channels (X: Perp., Y: Paral., Z: Polar and Refl.) with $\mathbf{H}_b$ along −/+Y axis. For a particular channel, the contrast is normalized to the maximum Kerr amplitude observed within that time series. Black/white corresponds to the dynamic magnetization lying in the −/+ z-direction, −/+ x-direction, and +/− y-direction for the polar, perpendicular, and parallel components, respectively. The Cartesian axes are defined within Figure 1(a) and shown above the columns in panels (b) and (c).

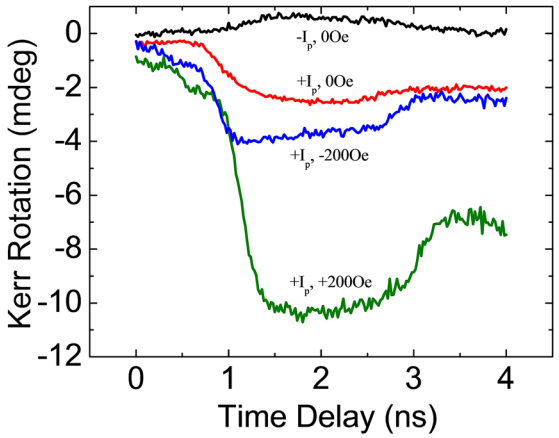

FIG. 5. Perpendicular component of the time resolved signal acquired at position A. The legend indicates whether the direction of the driving current is along +Y (+I_p) or −Y (–I_p) and whether the bias points +Y (+200 Oe) or −Y (−200 Oe).

indicating that the polar component is not affected by the direction of the bias field. Based upon the images recorded in the perpendicular and parallel channels, sketches of the putative equilibrium states that occur during the pulse cycling are presented in Figures 3(b) and 3(c). The 200 Oe bias field is insufficient to produce a uniform equilibrium state. A stripe domain pattern is still observed and the magnetization within the upper and lower parts of the yoke continues to cant in different directions. However when the bias field is along +Y direction, as in Figure 4(c), there are only three domains with anti-parallel magnetization within the yoke. Again the magnetization within the tip region does not simply follow the direction of the applied bias field, but occupies a meta-stable equilibrium state that is dependent on both the pulse polarity and the applied bias field. The blurriness of the dynamic images may indicate that the yoke dynamics are partly stochastic in character.

Figure 5 shows the perpendicular component of the time resolved signal acquired at position A in Figure 1(a), which is located deep in the confluence region, both with and without bias field and for driving currents of different polarities. When there is no bias field, the amplitude of the perpendicular magnetization component is greater when the driving current flows along +Y (red curve), but the magnetization relaxes less effectively after the current pulse has passed. When the current flows upwards, the response is larger when the bias field points to +Y (+200 Oe, blue curve) rather than −Y (−200 Oe, green curve), and the response is larger rather than without the bias field. This behavior is consistent with the contrast seen within the tip region for the perpendicular channel in Figures 4(b) and 4(c) and confirms that the direction of the applied bias field has a significant effect upon the dynamics of the writer. Since position A is close to the air bearing surface (ABS), it seems likely that very different head fields will be obtained by changing the polarity of either the driving current or the bias field. The perpendicular magnetization component does not appear to relax fully after the current has passed for any of the four curves, suggesting that EAW may be a significant problem.

In summary, the magnetization dynamics within a multilayered writer yoke have been clearly resolved in TRSKM measurements. The perpendicular and parallel channel dynamic images suggest that, in the absence of a bias field, the yoke supports a stripe domain equilibrium state while the equilibrium state of the tip during pulse cycling is metastable and depends upon the polarity of the driving current. A bias field of 200 Oe is insufficient to induce a uniform equilibrium state and a modified stripe domain configuration continues to be observed. The dynamics observed within the tip region suggest that the equilibrium state during repeated pulsing depends upon the polarity of both the driving current and the bias field. Different combinations of bias field and current polarity lead to different dynamics deep within the confluence region, in agreement with recent modeling work.[15] These data suggest that the magnetization dynamics throughout the yoke can vary significantly depending on the current polarity and any bias or anisotropy field.

The authors gratefully acknowledge financial support from the Seagate Plan.

[1]O. Heinonen, A. Nazarov, and M. L. Plumer, J. Appl. Phys. **99**, 08S302 (2006).
[2]F. H. Liu and M. H. Kryder, J. Appl. Phys. **75**, 6391 (1994).
[3]J. J. Kim, K. Hirata, Y. Ishida, D. Shindo, M. Takahashi, and A. Tonomura, Appl. Phys. Lett. **92**, 162501 (2008).
[4]P. Czoschke, S. Kaka, N. J. Gokemeijer, and S. Franzen, Appl. Phys. Lett. **97**, 242504 (2010).
[5]M. R. Freeman and J. F. Smyth, J. Appl. Phys. **79**, 5898 (1996).
[6]A. Taratorin and K. Klaassen, IEEE Trans. Magn. **42**, 157 (2006).
[7]T. Arnoldusse, C. Vo, M. Burleson, and J.-G. Zhui, IEEE Trans. Magn. **32**, 3521 (1996).
[8]K. Klaassen and J. C. L. van Peppen, IEEE Trans. Magn. **31**, 2657 (1995).
[9]X. Xing, A. Taratorin, and K. B. Klaassen, IEEE Trans. Magn. **43**, 2181 (2007).
[10]D. Z. Bai, J. Zhu, P. Luo, K. Stoev, and F. Liu, IEEE Trans. Magn. **42**, 473 (2006).
[11]P. Gangmei, P. S. Keatley, W. Yu, R. J. Hicken, M. A. Gubbins, P. J. Czoschke, and R. Lopusnik, Appl. Phys. Lett. **99**, 232503 (2011).
[12]M. Mallary, J. Appl. Phys. **57**, 3952 (1985).
[13]M. R. Freeman, G. M. Steeves, G. E. Ballentine, and A. Krichevsky, J. Appl. Phys. **91**, 7326 (2002).
[14]P. S. Keatley, V. V. Kruglyak, R. J. Hicken, J. R. Childress, and J. A. Katine, J. Magn. Magn. Mater. **306**, 298 (2006).
[15]Z. Li, D. Z. Bai, E. Lin, and S. Mao, J. Appl. Phys. **111**, 07B713 (2012).